Atmospheric Research 195 (2017) 31–43

Contents lists available at ScienceDirect

Atmospheric Research

journal homepage: www.elsevier.com/locate/atmosres

The relationship of lightning activity and short-duration rainfall events during warm seasons over the Beijing metropolitan region

Fan Wu[a,b], Xiaopeng Cui[b,c,*], Da-Lin Zhang[d,e], Lin Qiao[f]

[a] Key Laboratory of Cloud-Precipitation Physics and Severe Storms (LACS), Institute of Atmospheric Physics, Chinese Academy of Sciences, Beijing, China
[b] University of Chinese Academy of Sciences, Beijing, China
[c] Collaborative Innovation Center on Forecast and Evaluation of Meteorological Disasters, Nanjing University of Information Science & Technology, Nanjing, China
[d] Department of Atmospheric and Oceanic Science, University of Maryland, College Park, MD, USA
[e] Key State Laboratory for Severe Weather, Chinese Academy of Meteorological Sciences, China Meteorological Administration, Beijing, China
[f] Beijing Meteorological Bureau, China Meteorological Administration, Beijing, China

ARTICLE INFO

Keywords:
Lightning
Precipitation
Total lightning activity
Short-duration rainfall event
SAFIR-3000
Beijing

ABSTRACT

The relationship between lightning activity and rainfall associated with 2925 short-duration rainfall (SDR) events over the Beijing metropolitan region (BMR) is examined during the warm seasons of 2006–2007, using the cloud-to-ground (CG) and intracloud (IC) lightning data from Surveillance et Alerte Foudre par Interférometrie Radioélectrique (SAFIR)-3000 and 5-min rainfall data from automatic weather stations (AWSs). An optimal radius of 10 km around selected AWSs is used to determine the lightning-rainfall relationship. The lightning-rainfall correlations vary significantly, depending upon the intensity of SDR events. That is, correlation coefficient ($R \sim 0.7$) for the short-duration heavy rainfall (SDHR, i.e., ≥ 20 mm h^{-1}) events is found higher than that ($R \sim 0.4$) for the weak SDR (i.e., 5–10 mm h^{-1}) events, and lower percentage of the SDHR events ($< 10\%$) than the weak SDR events (40–50%) are observed with few flashes. Significant time-lagged correlations between lightning and rainfall are also found. About 80% of the SDR events could reach their highest correlation coefficients when the associated lightning flashes shift at time lags of < 25 min before and after rainfall begins. Those events with lightning preceding rainfall account for 50–60% of the total SDR events. Better lightning-rainfall correlations can be attained when time lags are incorporated, with the use of total (CG and IC) lightning data. These results appear to have important implications for improving the nowcast of SDHR events.

1. Introduction

Lightning and precipitation are two typical phenomena that frequently co-occur in thunderstorms. The relationship between lightning activity and precipitation has been noticed for very long, but the physical basis between the two was studied only during the past few decades. For example, previous studies of both laboratorial experiments (Jayaratne et al., 1983; Saunders and Brooks, 1992; Saunders and Peck, 1998; Takahashi, 1978; Williams et al., 1991) and field observations (Carey and Rutledge, 1996, 2000; Williams et al., 1989) have reported that the non-inductive charging mechanism may be the main electrification process in continental convective storms. This mechanism indicates that the initiation of lightning is in a mixed-phase environment with graupel/hail, ice crystal and supercooled water, which is closely related to cloud ice microphysical processes. Therefore, a positive relationship between lightning and precipitation may be expected in storms with vigorous ice-phase processes. With the development of lightning detection technology, more detailed lightning observations can be obtained, which helps markedly quantify the relationship between lightning and rainfall. Some previous studies demonstrated that the lightning-rainfall relationship could provide valuable information about the improvements in heavy-rain nowcasts and short-term severe weather warnings (Koutroulis et al., 2012; Price and Federmesser, 2006; Soula et al., 1998; Tapia et al., 1998) and in the estimation of rainfall amount (Garcia et al., 2013; Soula and Chauzy, 2000; Tapia et al., 1998; Xu et al., 2013, 2014). Hence, more thorough studies of the lightning-precipitation relationship are of great significance.

A growing number of studies have shown much interest in examining the lightning-rainfall relationship associated with rainfall events.

* Corresponding author at: Key Laboratory of Cloud-Precipitation Physics and Severe Storms (LACS), Institute of Atmospheric Physics, Chinese Academy of Sciences, Beijing 100029, China.
E-mail address: xpcui@mail.iap.ac.cn (X. Cui).

http://dx.doi.org/10.1016/j.atmosres.2017.04.032
Received 11 December 2016; Received in revised form 11 March 2017; Accepted 11 April 2017
Available online 13 May 2017

Piepgrass et al. (1982) found a trend of lightning occurring prior to precipitation in two thunderstorms in central Florida, in which the best *Rs* of 0.79 and 0.93 were achieved when lightning was delayed by 4 and 9 min, respectively. Soula and Chauzy (2000) found that spatial correlations between rainfall and lightning are consistent for all lightning types, and positive CG flashes are better associated with rainfall amounts than negative flashes. Koutroulis et al. (2012) studied 16 rainfall events (4 flood plus 12 non-flood events) over the island of Crete, and found that a higher correlation is obtained within 15 km around the station and an average time lag that lightning preceded rainfall of 15 min. Katsanos et al. (2007) studied rainfall events in the central and eastern Mediterranean using 6 hourly rain-gauge accumulated rainfall data and CG lightning data, and found that lightning-rainfall correlations differ, depending on rainfall amount. That is, more than half of the rainfall events without flashes are accompanied with small 6-h accumulated rainfall amounts (≤ 1 mm), while only 6% of them produce large rainfall amounts (> 10 mm). In contrast, only 17% of the rainfall events with flashes could be considered as weak rainfall events and 30% of them as intense rainfall events. Iordanidou et al. (2016) investigated the lightning-rainfall relationship over Crete Island using 22 rain-gauge data and lightning data of CG plus some IC flashes, and found that the mean lightning-rainfall *R* could reach 0.6 within a radius of 25–30 km from the center of each lightning cluster. Higher correlations are obtained for more intense rainfall and more flash counts within the searching area. Feng et al. (2007) studied 10 hailstorms based on CG and total lightning data, radar reflectivity and microphysics data from TRMM satellite, and found a good correlation between ice water content (*IWC*) and flash rates, with an *R* of 0.69. Their results revealed the critical roles of ice precipitation particles in determining the electrical process of thunderstorms. Matthee et al. (2014) discovered quantitative differences between lightning and non-lightning convective rainfall events using polarimetric radar and satellite data. Namely, stronger updrafts are observed in thunderstorms than those in non-lightning storms, accounting for the formation of deeper clouds with more ice particles in the mixed-phase regions. Apparently, the previous studies have provided enough evidence for positive correlations between lightning and rainfall, and for lightning activity to usually precede rainfall with a time lag of a few minutes. Therefore, lightning information has the potential to become an effective tool for nowcasting rainfall events.

Likewise, considerable work has been conducted to study the short-duration rainfall (SDR) events, usually defined as those lasting for ≤ 6 h in duration, generally using hourly precipitation data (Feng et al., 2007; Li et al., 2008; Yang et al., 2013; Yu et al., 2007; Yuan et al., 2014). Previous studies show that short-duration heavy rainfall (SDHR) events frequently induce flash floods, urban waterlog disaster, landslide and many other losses (Brooks and Stensrud, 2000; Yuan et al., 2014). Globally, climatological studies show an increasing probability of heavy rainfall events around the world in the past decades under the influence of global warming (Groisman et al., 2005; Min et al., 2011; Trenberth, 2011; Zhai et al., 2005). Locally, the Beijing metropolitan region (BMR) suffers frequently from SDHR events in recent decades, such as the 21 July 2012 torrential rain (Zhang et al., 2013). Thus, studying SDR events over the BMR is of great importance. Li et al. (2008) used hourly precipitation data during 1961–2004 to study climatological characteristics and secular trends of summer precipitation in the BMR, and found that while the total rainfall amount of long-duration events has decreased, that of SDR events has increased significantly. In addition, SDR events occur often from late afternoon to early morning hours. This finding was later confirmed by Wang and Wang (2013), who used 5-min rainfall data from 187 high-density Automatic Weather Stations (AWSs) in the BMR during the warm season of 2006–2010. Using the similar rainfall data, Yang et al. (2013) indicated that the frequency and amount of summer rainfall are mainly determined by the SDR events with 1–3 h duration, and most of the rainfall amounts occur in the events with duration of < 6 h. The dominant contributions of the SDR events have also been noted by Yuan et al. (2014), who analyzed the topographic effects on spatialtemporal variations of SDR events during the warm season of the central North China (NC), using the hourly rainfall records of 2005–2012. Wu et al. (2000) found different trends of SDHR events between urban areas and suburbs of the BMR, with significantly more and stronger events over the urban areas.

Despite the numerous studies of SDR events as mentioned above, little attention has been paid to their relationship with lightning activity, especially given the availability of rainfall observations at 5-min intervals over the BMR. Moreover, while many previous studies showed high lightning-rainfall correlations associated with individual thunderstorms, it is not possible to obtain a quantitative relationship between rainfall amounts and flash counts in each rainfall event (Katsanos et al., 2007). This is mainly because lightning is more closely correlated with convective precipitation, and most rainfall events examined by many of the previous studies may also contain stratiform rainfall with lower rates. Could the lightning-rainfall relationship be refined by grouping SDR events into different rainfall-rate grades in order to differentiate between convective and stratiform rainfall? In particular, given the currently available 5-min rainfall data, is it possible that certain percentages of the SDR events precede, lag behind or coincide with lightning activity, respectively? As the total lightning (CG and IC) data are shown more robust correlation to severe weathers (Chronis et al., 2015; Schultz et al., 2011), are the total lightning data correlated better to rainfall than CG lightning data? Thus, it is our intention to address the above questions by studying the lightning-rainfall relationship associated with SDR events during the warm seasons (May–September) of 2006–2007 using 5-min precipitation data from 118 AWSs in the BMR and Surveillance et Alerte Foudre par Interférometrie Radioélectrique (SAFIR)-3000 lightning data (including both CG and IC lightning). The SDR events are analyzed herein because of their dominance during the warm seasons and the much needed effort in improving their predictability (Zhang et al., 2015). Using the grouping methods, the correlations of lightning and rainfall are discussed in different classifications, including the SDR events with different intensity grades. From the calculations of time-lagged correlations, the percentages of the SDR events precede, lag behind or coincide with lightning activity could be quantified. Besides, the lightning-rainfall correlations are examined and compared by the using the CG and total lightning data provided by the SAFIR-3000 lightning system.

The next section describes the data source and methodology used for this study. Some logics to calculate various lightning-rainfall correlations are also described. Section 3 presents the calculations of lightning-rainfall relationship, with different time-lagged windows. A summary and concluding remarks are given in the final section.

2. Data and methodology

2.1. Datasets and quality control

2.1.1. Lightning data

Both the CG and IC lightning data used in this work are obtained from Beijing's SAFIR-3000 lightning location network, which consists of three stations and covers a detection area of 270–280 km^2 over the BMR (Fig. 1a). The SAFIR-3000 system is a three-dimensional multi-station detection system providing the timing, location and polarity of both CG and IC lightning flashes. Each station has a very-high-frequency (VHF) sensor (110–118 MHz) and a low-frequency (LF) sensor (300 Hz–3 MHz) to discriminate between CG and IC lightning. The best detection area is located inside the triangle defined by the three stations with the detection efficiency of $> 90\%$ and the location errors of < 2 km (Zheng et al., 2009).

The SAFIR-3000 system detects radiation sources from lightning flashes. One lightning flash usually produces one or more radiation sources. In order to determine the number of flashes, a data quality control is performed, following Novák and Kyznarová (2011) and Liu

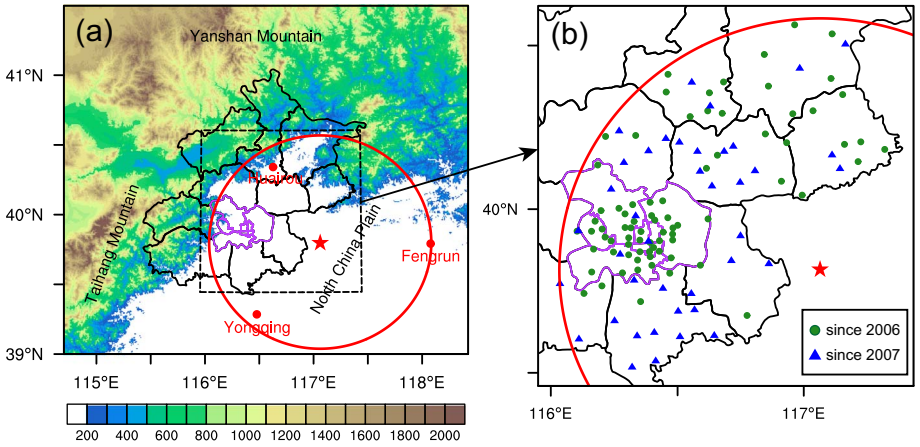

Fig. 1. (a) Locations of the three SAFIR-3000 stations (red dots) and topography (shaded, m) over the BMR and its adjacent areas. Black lines denote the geographical boundaries of the BMR, with its urban area indicated by purple lines. The best detection area of the SAFIR-3000 is indicated by a red circle with a radius of 100 km from the center (red star) of the three stations. Panel (b) is a zoomed-in area of the dashed rectangle in (a), and shows the spatial distribution of the AWSs used in this study. Green points indicate the locations of AWSs in the best detection area of the SAFIR-3000 since 2006, and the blue triangles indicate those built since 2007. (For interpretation of the references to color in this figure legend, the reader is referred to the web version of this article.)

et al. (2013). That is, radiation sources within 1 s and at a distance of < 10 km are defined as one IC flash. In addition, we have removed (a) IC flashes below 1 km, based on previous observations in the NC showing few IC flashes; and (b) IC flashes at an altitude higher than 18 km, in accordance with pervious radar observations that cloud tops over the BMR seldom exceed 16 km altitude (Liu et al., 2013). First return strokes are also used with the 1-s and 10-km method to define CG flashes, and positive CG flashes with the peak current of < 10 kA are considered as IC flashes (Poelman, 2014; Taszarek et al., 2015).

2.1.2. Rainfall data

Rainfall data at 5-min intervals, acquired from Beijing's AWSs network, cover an area that is much larger than the effective detection area of the SAFIR-3000 network. Thus, only the AWSs in the most effective range of 100 km from the center of individual SAFIR-3000 stations are used in the analysis (Wu et al., 2016). The number of the selected AWSs in the overlapped region has increased from 78 to 118 during 2006–2007 (Fig. 1b). The quality control of the rainfall data consists of internal consistency test, climatological extreme value test and time consistency test, following Wang and Wang (2013). Specifically, as the rainfall data are recorded as the accumulated rainfall amount at the beginning of every hour at 5-min intervals, the 5-min accumulated rainfall amount has to be computed first from the difference of the current record and the previous one, so any negative value in rainfall rate will be eliminated for internal consistency. Second, any 5-min accumulated rainfall amount exceeding 30 mm is considered as false data and removed. Third, every rainfall record > 0.1 mm should have continuous data 1 h before and after.

With the 5-min rainfall data, we define an SDR event at individual stations, following Wang and Wang (2013). An SDR event begins when both 5-min rainfall ≥ 0.1 mm and its subsequent 1-h accumulated rainfall ≥ 5 mm are held, and this time is defined as the starting time of the event (T_{start}). This event ends when the subsequent 1-h accumulated rainfall becomes < 5 mm, and this time is defined as the ending time of the event (T_{end}). Thus, the duration of this SDR event is defined as $T_{sus} = T_{end} - T_{start}$. Based on the 1-h accumulated rainfall after T_{start}, SDR events could be categorized into six grades (see Table 1), and an SDHR event is defined as the one with the hourly rainfall rate (HRR) of ≥ 20 mm after T_{start} (Wang and Wang, 2013). As a result, a total of 2925 SDR events are identified, in which 1443, 928, and 554 events are categorized as weak (i.e., 5–10 mm h^{-1}), moderate (i.e., 10–20 mm h^{-1}), and intense (≥ 20 mm h^{-1}) ones, respectively (Table 1).

2.1.3. Optimal radius to count lightning flashes

To analyze the relationship between lightning activity and SDR events, the corresponding CG and total flashes must be counted in 5-min intervals at the AWSs. Typically, lightning flashes within a certain radius of a station are often counted in the same time intervals as rainfall records (Barnolas et al., 2008; Koutroulis et al., 2012; Michaelides et al., 2010). Previous studies show higher lightning-rainfall correlations could be found within the radii of 6–30 km (Barnolas et al., 2008; Iordanidou et al., 2016; Katsanos et al., 2007; Koutroulis et al., 2012; Michaelides et al., 2010). Because of little guidance for the correlations in SDR events by using 5-min rainfall data, some efforts will be devoted in Section 3.1 to determine the optimal radius at which the highest mean lightning-rainfall correlation coefficient (R) could be obtained. To determine at what radius higher lightning-rainfall correlations could be found, a group of radii ranging from 2 to 30 km at 2-km intervals and 30–60 km at 5-km intervals are tested, and then the mean lightning-rainfall Rs of all the 2925 SDR events in different radii are calculated. The optimal radius in determined when the mean R of all the SDR events could reach the highest value.

2.2. Calculations of the lightning-rainfall correlations

Like in the previous studies, the lightning-rainfall correlations in the SDR events need to be calculated. In this study, a mean and a peak rate of both flash counts and rainfall amounts in each SDR event are first computed. Then, the R's calculations for the 2925 events are performed in the mean and peak flash-rainfall pairs. Furthermore, the mean and peak flash rates are categorized into different bins to examine the variation of the mean (peak) rainfall rates with the mean (peak) flash rates. Likewise, the mean rainfall rates are categorized into different bins to study the variation of CG or total flash rates with the rainfall rates. Additional flashes associated with the SDR events which occurred outside of the duration of the SDR events (i.e., T_{sus}) are considered, and the time windows of 5–60 min at 5-min intervals before and after T_{sus} will be examined in Section 3.2.

Since numerous previous studies have noted that lightning activity usually precedes rainfall occurrences, with a time window ranging from a few minutes to nearly an hour (Koutroulis et al., 2012; Liu et al., 2011; Piepgrass et al., 1982; Tapia et al., 1998). Meanwhile, some studies pointed out that such temporal relationships between the two phenomena are complicated, and all the time-preceded, time-delayed or no-time-lag relationships between them could be found in different thunderstorms (Soula and Chauzy, 2000; Zheng et al., 2009). Therefore,

Table 1
The number and the percentage of the short-duration rainfall (SDR) events in six intensity grades that are obtained by analyzing the BMR's AWS rainfall observations in 5-min intervals during the warm seasons of 2006–2007.

	Weak	Moderate	Intense				
HRR ($mm\ h^{-1}$)	[5,10)	[10,20)	[20,30)	[30,40)	[40,50)	[50, + ∞)	Total
No. of events	1443	928	323	127	55	49	2925
Percentage (%)	49.3	31.7	11.0	4.3	1.9	1.8	100.0

Table 2
The strength of correlation according to Evans (1996).

Pearson correlation coefficient (R)	Strength of correlation
[0.0, 0.2)	Very weak
[0.2, 0.4)	Weak
[0.4, 0.6)	Moderate
[0.6, 0.8)	Strong
[0.8, 1.0)	Very strong

in order to clarify the temporal relationship in our SDR events, the lagged correlation (i.e., the correlation between the time-shifted series of lightning and rainfall) will be examined in Section 3.3, with the time lags ranging from − 60 to 60 min at 5-min intervals. Then the highest lagged R for each event in the different time lags will be used to evaluate how well the lightning-rainfall correlation could reach.

To determine the strength of the above-mentioned correlations, Evans' (1996) suggested values, as given in Table 2, are used by applying Pearson's R to the statistical analyses of the no-zero pairs of flash and rainfall, where R has a value between + 1 and − 1, with a positive (negative) value indicating a positive (negative) correlation; a zero value means that no linear correlation between the two variables occurs. The higher absolute value of R is, the stronger the linear correlation reaches. When R is calculated from no-zero flash-rainfall pairs in each SDR event, the pairs during T_{sus} and within 1 h before and after T_{sus} are included in the calculation. If all the values of flash or rainfall time series are zero, no linear correlation between them will be obtained (i.e., $R = 0$). Similar methods are used for the time-lagged correlations.

2.3. Statistical hypothesis tests

To determine the uncertainty of the results, hypothesis tests are performed for the single R and the difference of mean Rs. Methods of the hypothesis tests are summarized below.

2.3.1. Hypothesis test for correlation coefficient

The hypothesis for R is to examine whether or not a linear correlation exists between the two variables. Under the null hypothesis (H_0) of no linear correlation (e.g., $\rho = 0$), the test statistic

$$t_0 = \sqrt{n-2}\,\frac{R}{\sqrt{1-R^2}} \tag{2.1}$$

follows a distribution of the Student's (t) distribution with (n − 2) degrees of freedom (n is sample size) (Siegert et al., 2017). Under the alternative hypothesis (H_A) that linear correlation exists between the two variables (i.e., $\rho \neq 0$), a two sided test is performed at the significance level α. Thus, the null hypothesis will be rejected at the α level if the test statistic t_0 is larger than the (1 − α/2) quantile or smaller than the (α/2) quantile of the t distribution.

2.3.2. Hypothesis test for differences of mean correlation coefficients

Whether or not the correlation of rainfall and total flashes is better than that of rainfall and CG flashes is examined in this work. For this, the differences of the mean Rs for the two correlations are tested. As the hypothesis test method for the difference of means between paired samples shown in Wilks (2006), the sample statistic of $\Delta = R_{ay} - R_{by}$ is used, with the sample mean

$$\overline{\Delta} = \frac{1}{n}\sum_{i=1}^{n}\Delta_i = \overline{R}_{ay} - \overline{R}_{by}. \tag{2.2}$$

Under the null hypothesis that $\mu_\Delta = 0$ (i.e., there is not significant difference between the two means), the test statistic is defined as

$$z = \frac{\overline{\Delta} - \mu_\Delta}{(s_\Delta^2/n)^{1/2}}, \tag{2.3}$$

where s_Δ^2 is the sample variance of Δ, and will be distributed as the standard Gaussian for large samples. Since the two kinds of Rs usually exhibit serial correlation, the sample size of n in Eq. 2.3 should be replaced by the effective sample size, which can be estimated using the approximation

$$n' \cong n\frac{1-\rho_1}{1+\rho_1}, \tag{2.4}$$

where ρ_1 is the correlation coefficient of R_{ay} and R_{by}.

3. Results

In this section, the optimal radius around the AWS to count lightning flashes in 5-min intervals is determined first. After that, the flash counts could be paired with the 5-min rainfall data. Then, the lightning-rainfall correlations associated with the SDR events are investigated, including the correlation between mean (peak) rainfall rates and mean (peak) flash rates as well as the variations of correlation coefficients (Rs) with different time windows. Finally, the time-lagged correlations between lightning and rainfall are analyzed, and their differences in the SDR events with different intensity grades are also discussed.

3.1. Determining the optimal radius for lightning-rainfall correlations

In general, the higher the mean R is, the better the radius tested performs. The results are given in Fig. 2, showing clearly an optimal radius of 10 km with the highest mean Rs for both CG and total lightning-rainfall correlations. It is shown that the mean Rs decline sharply with radius decreasing from the optimal radius of 10 km, because fewer flashes are involved in the R's calculations. By comparison, the mean Rs exhibit slow decreases with the increasing radius beyond 10 km due to more flashes unrelated involved. Therefore, the lightning flashes (CG or total) at the optimal radius of 10 km from the AWSs are counted to pair with the AWSs' 5-min rainfall records in this work.

3.2. The lightning-rainfall correlation

The correlations of lightning and rainfall are first analyzed from all the 2925 SDR events. It is shown that both the CG and total flash counts were positively correlated with rainfall, with the R of 0.47 and 0.46, respectively (Fig. 3a and c). Statistical hypothesis tests for the R at the

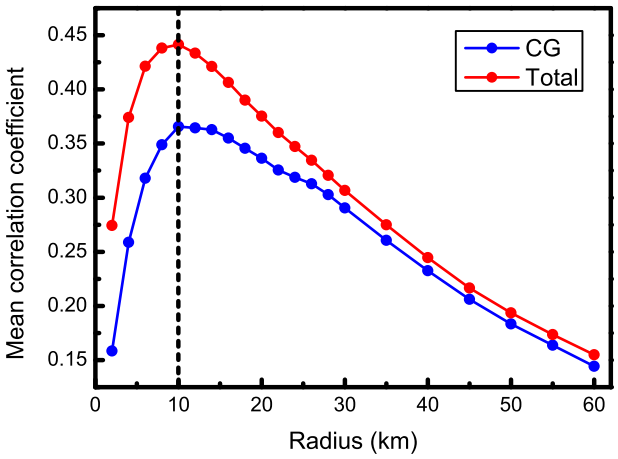

Fig. 2. Variations of the mean correlation coefficient between CG (total) flash and rainfall of all the short-duration rainfall (SDR) events in radius around the AWSs ranging from 5 to 60 km, as denoted by blue (red) line. (For interpretation of the references to color in this figure legend, the reader is referred to the web version of this article.)

significant level $\alpha = 0.05$ show that with the sample size $n = 2925$, the test statistics t_0 are 28.62 and 28.37, respectively, both exceeding the 97.5th percentile value of 1.96 with 2923 degrees of freedom in the t distribution. Therefore, the H_0 that the CG (total) flash has no linear correlation with rainfall amount would be rejected, and the CG (total) flash is significantly correlated to the rainfall amount at the 5% level. The SDR events with larger rainfall amounts are exhibited to be better correlated with flash counts. In contrast, the SDR events with small rainfall have flash counts with higher variations and distribute more away from the best fitting lines. Similarly, the peak CG (total) flash rate and peak rainfall rate also exhibit positive correlations with the R of 0.38 (0.40), and the hypothesis tests show the correlations significantly exist at the 5% level. (Fig. 3b and d). The correlation of lightning flashes and rainfall amounts is difficult to see from the scatter plots as given in Fig. 3, due to the high variations of samples. To see the correlations more clearly, the lightning flash data or rainfall data are grouped into different bins, and then the tendencies of the bins are examined. Previous studies also indicate that lightning-rainfall correlations are usually influenced by the time shifts between the lightning flash and rainfall serials (Koutroulis et al., 2012; Soula and Chauzy, 2000). So the variations of lightning-rainfall correlations in different time windows are also examined below based on the grouped bins.

All the mean rainfall rates of the SDR events are grouped into bins according to the events' mean flash rates, and then the medians of mean rainfall (flash) rates in the bins are computed. The result is given in Fig. 4a and c, showing that the medians of mean rainfall rates had a strong positive correlation with the medians of mean CG flash rates with $R = 0.74$, and even a stronger positive correlation with those of mean total flash rates with $R = 0.82$. Both the correlations are significant at the 5% level through the hypothesis tests. The scatters of the medians exhibit that the median of mean rainfall rates in the lowest mean-flash-rate bin deviates obviously from the best fitting line (Fig. 4a and c). This implies that it is not desirable to take the SDR events with very small rainfall rates into the correlation analysis. Because small rainfall rates mainly occur in stratiform clouds with little lightning activity, whereas higher rainfall rates are often found in convective precipitation that is correlated closely with lightning activity (Petersen and Rutledge, 1998). Similarly, when all the peak rainfall rates in the SDR events are grouped into bins according to the events' peak flash rates, the medians of the peak rainfall rates also show a high positive correlation with the medians of the peak flash rates, namely a correlation of $R = 0.79$ with the peak CG flash rates and $R = 0.92$ with the peak total flash rates. And both the correlations are

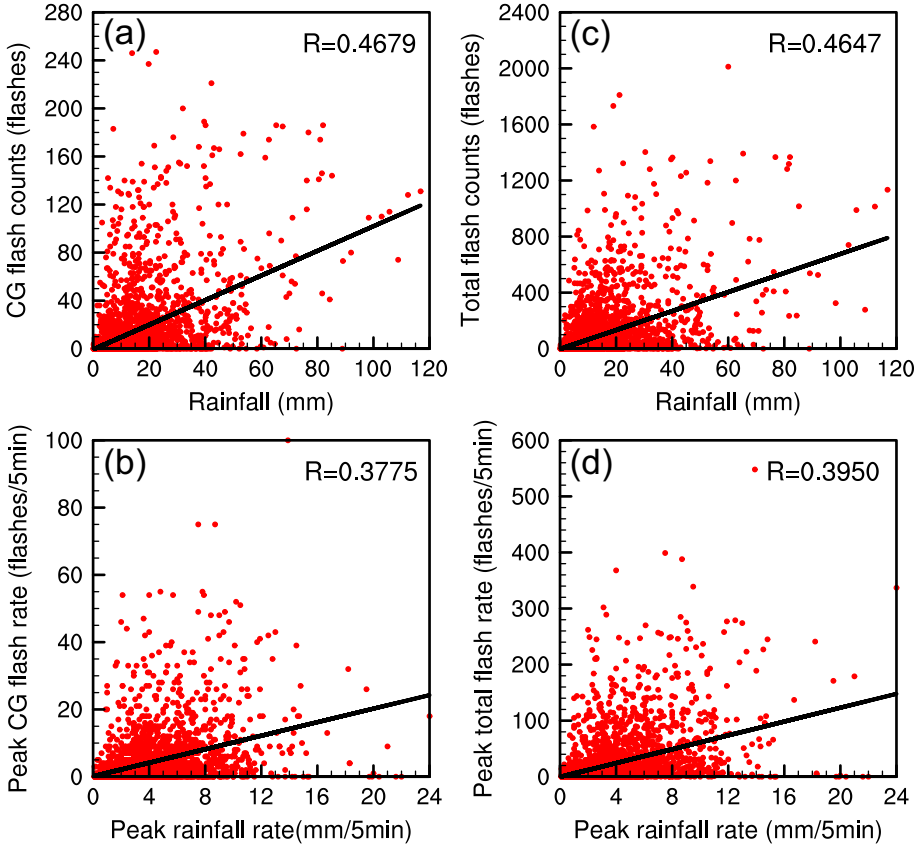

Fig. 3. Scatter plots of the (a) CG and (c) total flash counts (flashes) as a function of rainfall (mm) in the SDR events; and of the peak (b) CG and (d) total flash rates [flashes (5 min)$^{-1}$] as a function of the peak rainfall rate of the SDR events [mm (5 min)$^{-1}$]. Black lines denote the best fitting lines.

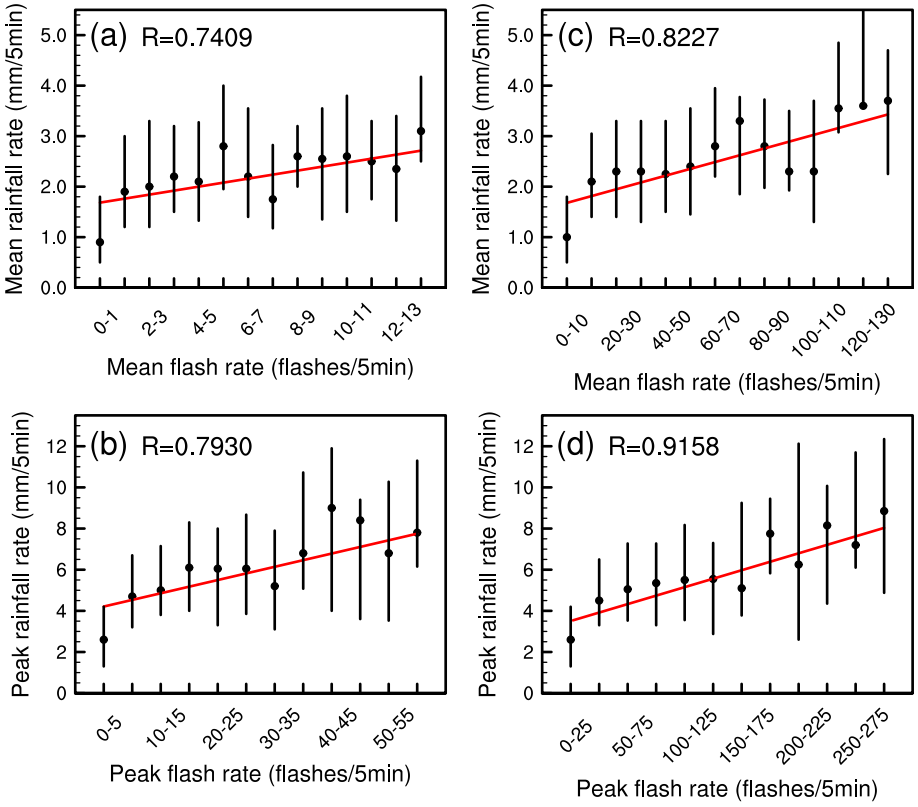

Fig. 4. Mean rainfall rates [mm (5 min)$^{-1}$] as a function of mean-flash-rate bins [flashes (5 min)$^{-1}$] in the SDR events for (a) CG and (c) total lightning. Scatters denote the median of mean rainfall rate and the whiskers denote the rainfall rate data extended from lower to upper quartiles. Panels (b) and (d) are the same as (a) and (c), respectively, but for the peak rainfall rates [mm (5 min)$^{-1}$] as a function of the peak flash rates [flashes (5 min)$^{-1}$].

significant at the 5% level. It is shown that the total lightning flashes could have a better correlation with rainfall than the CG flashes.

The mean and peak flash rates in each SDR event discussed above are computed within T_{sus}, but lightning activity often occurs with some time shifted either before or after T_{sus} (Koutroulis et al., 2012; Soula and Chauzy, 2000). So better lightning-rainfall correlation may be expected when wider time windows than T_{sus} are considered to compute the mean (peak) flash rates of the SDR events. Thus, we examine below the lightning-rainfall correlation in different time windows ranging from 5 to 60 min before and after. Using the same statistical methods mentioned above (i.e., Fig. 4), the R between the medians of mean (peak) flash rates and the medians of mean (peak) rainfall rates is computed, together with its variation with time windows. The result shows that the lightning-rainfall correlation varies significantly with the time windows, and that a better correlation could be obtained when wider time windows are used (Fig. 5) (all the correlations are significant at the 5% level). It is apparent from Fig. 5 that the R between the mean CG flash rate and mean rainfall rate has two major peaks in the time windows, which first peaks in the time window of 5 min, and then decreases to a minimum in 10 min, followed by a secondary peak in 20 min. After 20 min, R does not change much. Similarly, the R between the total flash rate and rainfall rate also has two peaks and one minimum, except that the secondary peak occurs in a wider time window of 35 min. The obvious variations of Rs indicate that there are considerable flashes before or after the T_{sus} of the SDR events. And the better correlation so obtained could be attributed to the wider time windows which involve more flash counts related in the computation of the mean flash rates. For example, when extra flash counts (CG or total) before and after 5 min of T_{sus} associated with the SDR events are considered, the SDR events could be grouped into bins with higher mean (CG or total) flash rates than those obtained by using T_{sus} shown in Fig. 4. The new grouping caused by the wider time windows is called the “regrouping process” in this work.

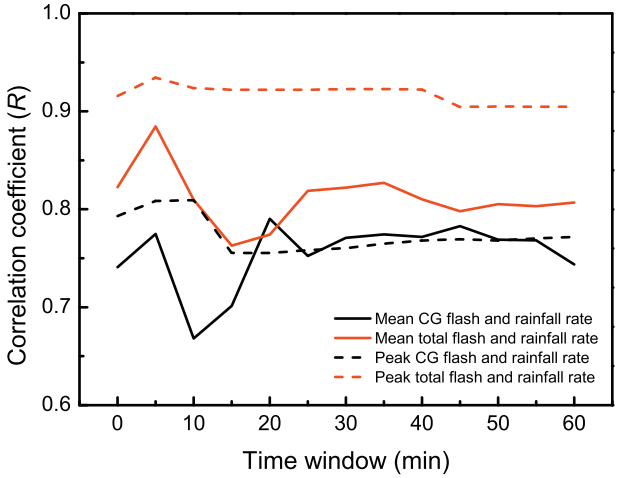

Fig. 5. Variations of the correlation coefficient (R) between the median of mean rainfall rate and the median of mean CG (total) flash rate, denoted by the black (red) solid line, and of the R between the median of peak rainfall rate and that of peak CG (total) flash rate, denoted by black (red) dashed line, with the time windows of 0–60 min. (For interpretation of the references to color in this figure legend, the reader is referred to the web version of this article.)

The analysis of Fig. 5 also indicates that lightning activity often occurred beyond T_{sus} of the SDR events, and better correlation between CG (total) flash rates and rainfall rates could be obtained when extra flash counts related are considered. The two peaks of Rs between the mean CG (total) flash rate and mean rainfall rate implies that some SDR events had lightning activity within the time window of 5 min, whereas some others had considerable CG (total) flash counts within the wider time window of 20 (35) min. Moreover, the total flash counts could provide wider time windows (e.g., 35 min) than the CG flash counts,

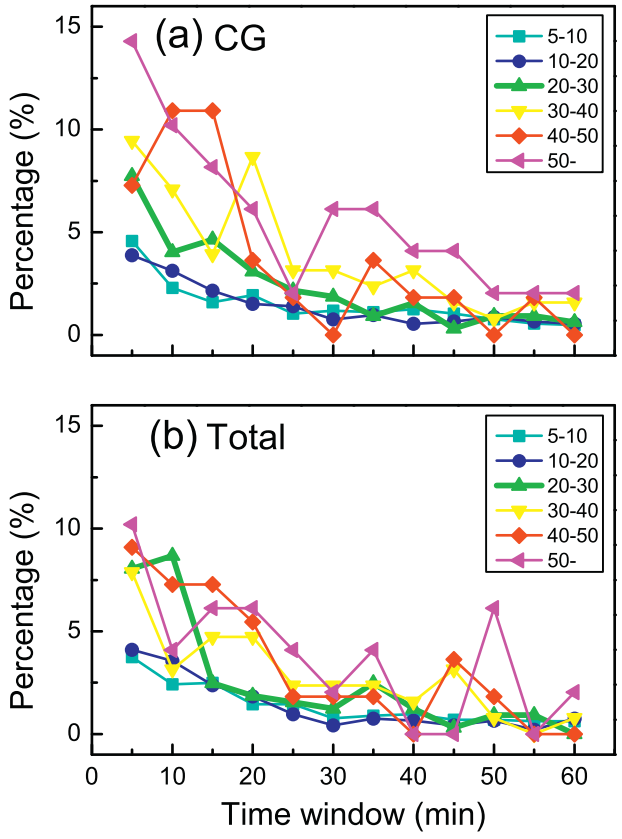

Fig. 6. Percentages of the regrouped SDR events in different intensity grades as a function of the time windows (min) for (a) CG, and (b) total flashes.

suggesting that the former could be more useful than the latter for guiding the nowcasts of SDR events. Similar results can be obtained for the correlation between the peak flash rate and peak rainfall rate, except that only one peak is found in the time windows of 5–10 min. The result indicates that the peak flash rates of the SDR events mostly occurred within T_{sus} and 10 min before and after, and seldom occurred beyond 10 min of T_{sus}.

The variations of *Rs* with different time windows reflect that lightning activity had obvious time shift to rainfall in the SDR events. One possible reason is that rain drops needs some minutes to fall through the vertical columns from charged clouds aloft (Piepgrass et al., 1982). In order to gain more insight into the effects of the time shifts on the lightning-rainfall correlation, further analyses of the SDR events with different grades are performed. First, Fig. 6a shows that the highest percentages of the regrouped SDR events with respect to the mean CG flash rates occur in the time window of 5 min, and that most of percentages have a secondary peak in the 10–20 min window. The results are consistent with those shown in Fig. 5. Although the SDR events with the rainfall rates > 40 mm h^{-1} had another peak in the time window of 35 min, they had little influence on the variation of the correlation between the mean CG flash rate and mean rainfall rate (Fig. 5) due to their small proportion in the total events (Table 1). In addition, the SDHR (HRR ≥ 20 mm h^{-1}) events usually had both a major and a secondary peak in the time window of 15–35 min, indicating that the SDHR events could be predictable by the lightning flashes in the time windows. Similarly, most of the SDR events, after regrouping into the higher mean-total-flash-rate bins, show the largest percentage in the time window of 5 min, and SDHR events display one or two secondary peaks in the time window of 15–35 min (Fig. 6b). The result is consistent with the variations of the correlation between the mean total flash rate and the mean rainfall rate in these time windows as shown in Fig. 5, suggesting that the secondary peak in the *R* of total flash rate and rainfall rate is mainly caused by the regrouping process in the SDHR events. Moreover, more related total flash counts could be found in the time window of 45–50 min in the SDHR events (e.g., HRR ≥ 30 mm h^{-1}), which suggests further that total lightning flashes could provide more advancing time than CG lightning flashes to predict the occurrences of the SDHR events. It is understandable from the fact that stronger updrafts with large convective available potential energy (CAPE) associated with SDHR events tend to generate deeper convective clouds that is favorable for non-inductive charging process (Matthee et al., 2014), while startiform clouds with lower rainfall rate have less lightning-precipitation processes (Petersen and Rutledge,

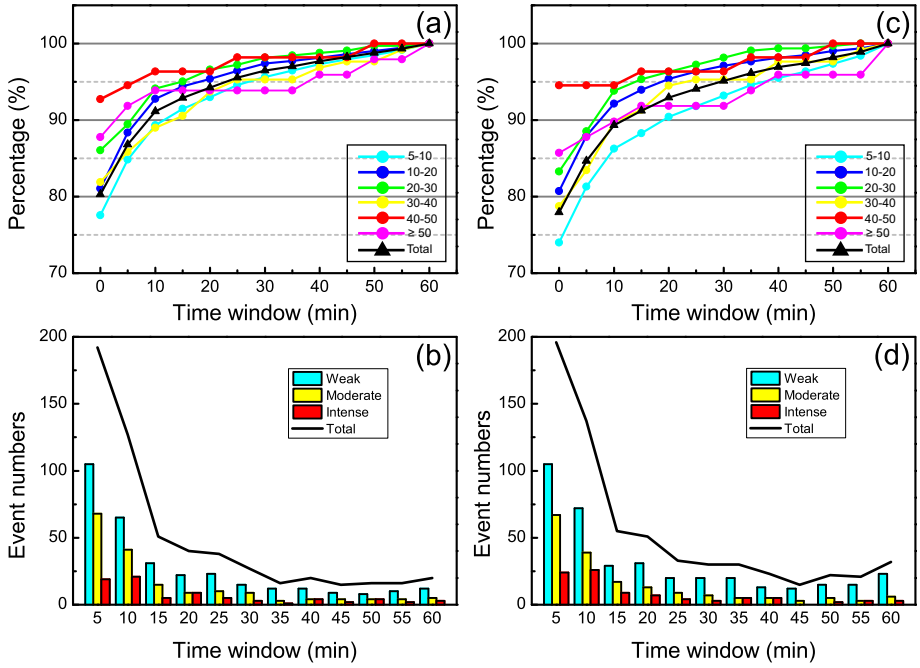

Fig. 7. Percentages of the SDR events in different intensity grades (mm h^{-1}) that could reach their peak (a) CG and (c) total flash rates [flashes (5 min)$^{-1}$] in the time windows of 0–60 min at the 5-min intervals; and numbers of the SDR events regrouped into higher (b) peak-CG-flash-rate bins or (d) peak-total-flash-rate bins in the time windows of 5–60 min at the 5-min intervals. Bars denote the regrouped SDR events with different intensity grades as shown in Table 1 and the black line denotes the total regrouped SDR events.

1998).

After discussing the time shift of mean flash rate for the SDR events, let us examine the time shift of the peak flash rate for the SDR events in different intensity grades. Fig. 7a and c show that nearly 80% of the SDR events could find their peak flash rates within T_{sus}, and the percentage increases quickly to nearly 90% in the time window of 15 min, and then grows slowly beyond. The peak flash rates beyond T_{sus} are more frequently found in the weak SDR events, whereas those within T_{sus} (i.e., in time window of 0 min) are mainly in the SDHR events. Compared with the peak CG flash rates, the percentages of the peak total flash rates are lower within T_{sus} for most of the SDR events (Fig. 7a and c), implying that the latter could be found more frequently than the former beyond T_{sus}. Due to the more flash counts of IC lightning considered, higher flash rates could be obtained by using total flashes, and more SDR events with peak flash rates long beyond T_{sus} may be found. When the peak flash rate beyond T_{sus} occurs, the SDR events would be regrouped into higher peak-flash-rate bins and the correlation between the peak flash rate and peak rainfall rate would be changed (Fig. 5). It is displayed in Fig. 7b and d that the regrouped SDR events mostly occurs within the time window of 10 min, indicating that the peak flash rates are usually found within 10 min before and after T_{sus}. In general, weak and moderate SDR events could be more frequently regrouped into higher peak-flash-rate bins, which is consistent with that shown in Fig. 7a and c. Furthermore, the rapid increase in the percentages of events with the peak flash rates (Fig. 7a and c) and the large amount of the regrouped events (Fig. 7b and d) in the time window of 5 and 10 min could explain the peak values of the R of peak flash rate and peak rainfall rate in Fig. 5.

To delve more into the lightning-rainfall relations, the mean rainfall rates of all the SDR events are stratified into different bins, as given in Fig. 8. It is shown that weaker lightning activity coincides with the SDR events with lower rainfall rates and longer durations [e.g., about 60 min at the mean rainfall rate of 0.5 mm $(5\ \text{min})^{-1}$]. The result means that mild and persistent precipitation typically associated with stratiform clouds produced less lightning flashes. With the increasing mean rainfall rate and the shortening duration, startiform precipitation gradually gives the way to convective precipitation in the SDR events, so the lightning flash rate goes up sharply. When the mean rainfall rate increases to 2.5 mm $(5\ \text{min})^{-1}$, the duration decreases to a minimum of 30 min but the flash rates continue their growths. This implies that the major precipitation type has changed from startiform to convective precipitation, and that the mean rainfall rate of 2.5 mm $(5\ \text{min})^{-1}$ could be used as a threshold for discriminating statiform from convective precipitation when the 5-min AWS rainfall data are used.

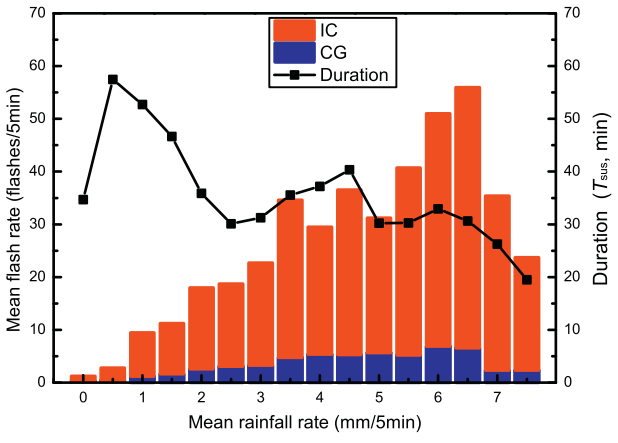

Fig. 8. Mean CG flash rates [blue stacked bars, flashes $(5\ \text{min})^{-1}$], mean IC flash rates [red stacked bars, flashes $(5\ \text{min})^{-1}$], and mean SDR event duration (T_{sus}) (black line, min) as a function of the mean rainfall rates [mm $(5\ \text{min})^{-1}$]. (For interpretation of the references to color in this figure legend, the reader is referred to the web version of this article.)

As the rainfall rate increases further to 4.5 mm $(5\ \text{min})^{-1}$, the duration of the SDR events reaches a secondary peak while the flash rate keeps increasing until reaching 6.5 mm $(5\ \text{min})^{-1}$, suggesting the intensification of convective precipitation. However, as the rainfall rate increases further to 7.0 mm $(5\ \text{min})^{-1}$, both the flash rate and duration exhibit apparent declines. This result indicates that in some extreme SDR events, lightning activity may not be as active as expected. Although this scenario is not previously reported frequently, it appears to be consistent with the microphysical budget study of Cui et al. (2015), who showed that some extreme rainfall categories are mainly contributed by warm-cloud processes (e.g., accretion of cloud water by rainwater) rather than ice-phase processes (e.g., melting of graupel). This result is also consistent with the work of Xia et al. (2015), who showed less CG lightning activity occurring in some nocturnal SDHR events due to the absence of large CAPE.

3.3. Time-lagged correlations

In this section, the time-lagged rainfall-CG flash and rainfall-total flash correlations in different time lags are discussed. The results are displayed in Figs. 9 and 10. Evidently, the means of all the lagged Rs roughly have a normal distribution centered near the time lag of zero. Moreover, the lagged rainfall-CG-flash R in the central time-lagged portion increases with more intense SDR events, e.g., the mean lagged R increases from 0.12 in events with HRR of 5–10 mm h^{-1} to > 0.50 in events with HRR of ≥ 50 mm h^{-1} events (Fig. 9). In each category of SDR events, the above time-lagged correlation decreases rapidly with ± time lags, and becomes negative as the time lag extends outward beyond ± 20 to ± 35 min from the weakest to the strongest SDR events. Of interest is that the best CG-flash-rain correlation occurs when lightning has a 5-min shift prior to rainfall in the events with 5–30 mm h^{-1} rainfall rates, but such a time shift does not occur in the SDR events with greater rainfall rates. By comparison, the lagged correlation between the total flash and rainfall rate, given in Fig. 10, appears to be better than the CG flash and rainfall rate correlation, because of the larger peak values of the mean R_S and their more centralized data distributions. In addition, all the SDR events exhibit a 5-min time lag that in shown in the CG-flash-rain correlation in the events with HRR of 5–30 mm h^{-1}, indicating again that the total lightning flash data could be more useful than the CG flash data for predicting the occurrences of SDHR events. To quantify the influence of the time lags on the time-lagged R, Fig. 11a and b show the percentages of SDR events that could reach their best time-lagged Rs in the time lags. We see that > 80% of the SDR events could reach the highest time-lagged R with respect to both the CG and total flashes, after making a 25-min time shift before and after their occurrences. The percentages of SDR events with CG or total lightning activity preceding, lagging or coinciding with rainfall, are given in Fig. 11c and d, showing that (i) in about 55% of the SDR events lightning flashes preceded rainfall; (ii) the SDR events with lightning flashes lagging behind rainfall accounted for about 30%; and (iii) the SDR events without any time shifts accounted for the remaining 15%.

In order to explore how the highest lightning-rainfall correlation could be reached for most of the SDR events, Fig. 12 shows the boxplots of the highest R in each SDR event in time lags from − 25 to + 25 min (accounting for > 80% of the SDR events). We see that if the lightning flash time series is shifted 25 min before or after the rainfall time series, a majority of the SDR events could reach high lightning-rainfall correlations (i.e., R = 0.6–0.8), and some SDR events could even reach very high correlations (i.e., R > 0.8). Of significance is that lightning flashes, especially the total flashes, are better correlated with rainfall in the SDHR events. In addition, Rs in the SDHR events with flashes preceding rainfall are higher than that in those with flashes lagging behind rainfall. The difference of the lightning-rainfall correlation for the SDR events with different intensity grades could be better seen from Table 3, showing that the weak SDR events had weak CG (total)

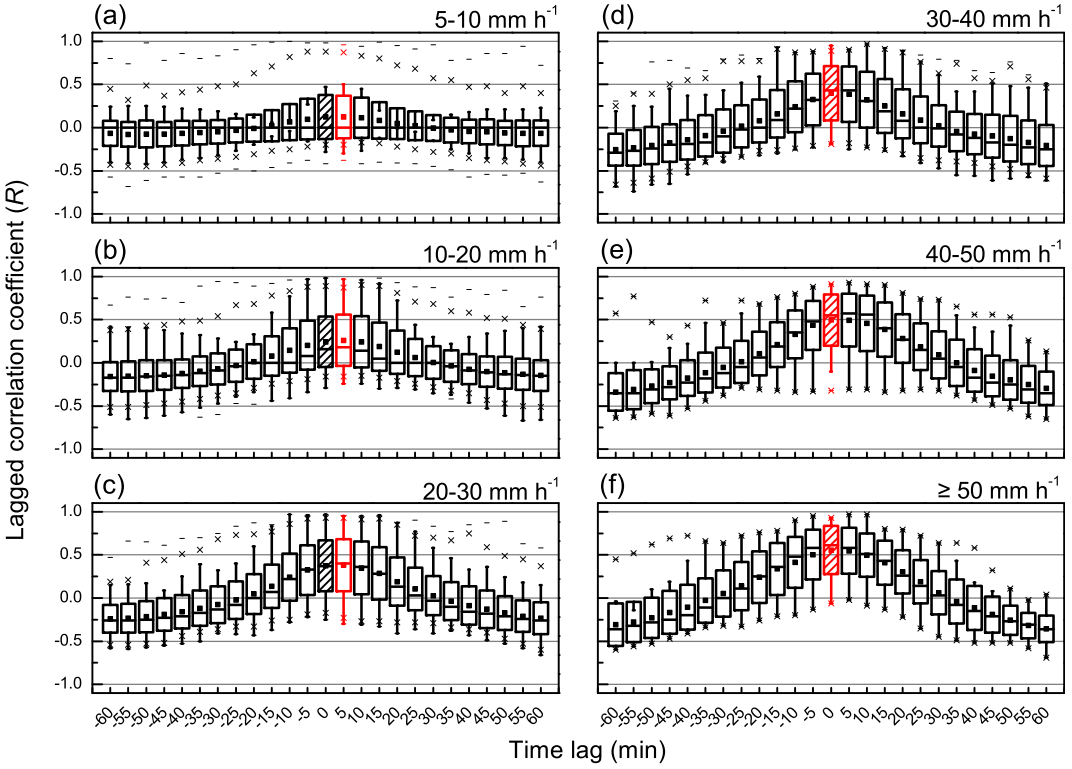

Fig. 9. Box plots of the time-lagged correlation coefficient between the CG flash and rainfall rates in the time lags of − 60–60 min. The cross-hatching box denotes the distribution of *R* with time lag of zero, and the red box denotes the time lag in which the highest mean *R* value is reached. (For interpretation of the references to color in this figure legend, the reader is referred to the web version of this article.)

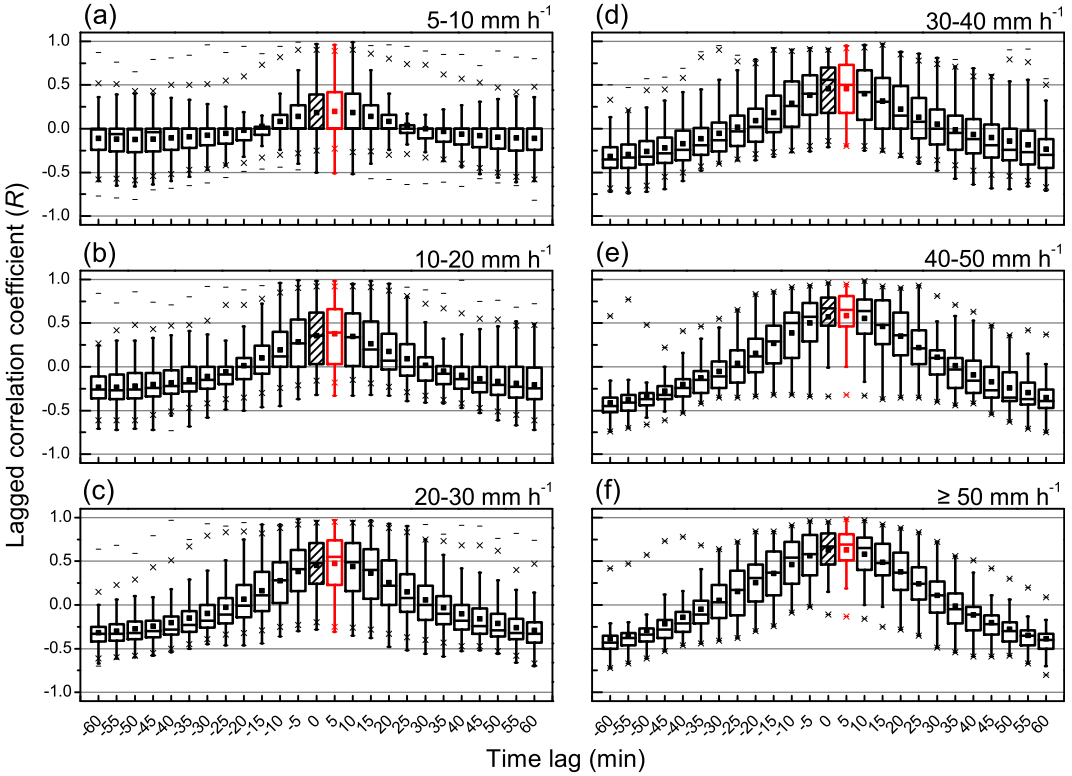

Fig. 10. As in Fig. 9, but for the time-lagged correlation coefficient between the total flash and rainfall rates.

lightning-rainfall correlation [i.e., $R = 0.32$ (0.40)], with about 50% (40%) of them accompanied with no CG (total) flashes. For the moderate SDR events, strong correlation could be found between total flashes and rainfall with $R = 0.62$, which is higher than that between CG flashes and rainfall. The percentage of no-total-flash SDR events is also lower than that of no-CG-flash ones. However, promising results of strong lightning-rainfall correlations are obtained in the SDHR events, and the *R* of CG (total) flashes and rainfall is 0.66 (0.73). Moreover,

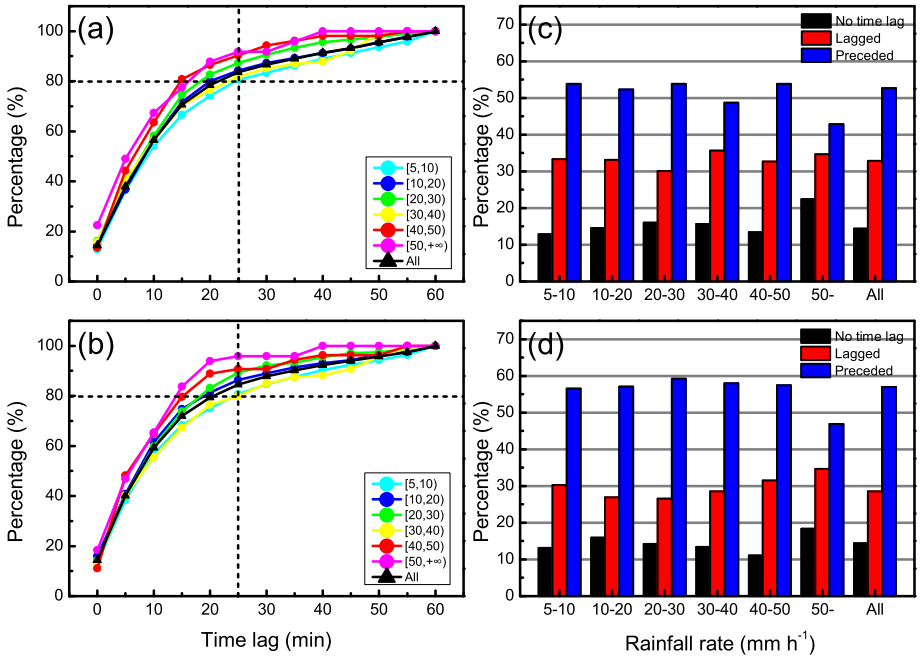

Fig. 11. Percentages of the SDR events that could reach their highest (a) rainfall-CG flash and (b) rainfall-total flash time-lagged *Rs* in the time lags of 5–60 min before and after T_{sus}; and percentages of the SDR events in which (c) CG flashes, and (d) total flashes preceded rainfall (blue bars), lagged behind rainfall (red bars) and had zero time lag with rainfall (black bars). (For interpretation of the references to color in this figure legend, the reader is referred to the web version of this article.)

much less no-flashes events are found in the SDHR events. Therefore, rainfall is more correlated to lightning flashes in the SDHR events. It is also shown in Table 3 that the *R* of total flashes and rainfall is higher than that of CG flashes and rainfall for the SDR events with different intensities. The difference of mean *R*s for the two correlations are tested, and the results show all the values of the test statistic *z* as given in Table 3 are higher than the 97.5th percentile value of 1.96 of the standard Gaussian distribution, which indicates that the correlation of total flashes and rainfall is significantly better than that of CG flashes and rainfall.

Finally, the spatial distributions of the mean highest *R* in different time lags are displayed in Fig. 13. Apparently, nearly all the AWSs with weak SDR events show weak or moderate correlations between CG (total) lightning flashes and rainfall (Fig. 13a and d). However, when the total flash data are used, the moderate SDR events could reach strong correlations ($R > 0.6$) at most the AWSs over the urban areas (Fig. 13b and e). Since the best correlation is associated with SDHR events, most AWSs with these events could have high lightning-rainfall correlations, and some AWSs could even have very strong correlations (Fig. 13c and f). In particular, the AWSs in the urban and northeastern mountainous areas all exhibited high or even very high lightning-rainfall correlations. Again, this confirms that shown in Figs. 4, 9, 10, 12 and Table 3 that the total lightning flashes are better correlated with rainfall than the CG flashes in the SDHR events.

4. Summary and concluding remarks

This paper analyzes the relationship between lightning and rainfall associated with a total of 2925 SDR events by using the SAFIR-3000 lightning data and 5-min rainfall data from 118 AWSs during the warm seasons of 2006 and 2007 over the BMR. To facilitate the analysis of the rainfall-lightning correlations, the SDR events are categorized into six different intensity grades according to their HRRs, and an optimal radius of 10 km from individual AWSs for counting their associated lightning flashes is used.

After grouping lightning flash rates and rainfall rates into different bins, an analysis of their correlations shows $R = 0.74$–0.82 between the mean rainfall rates and the mean flash rates, with higher values (i.e., $R = 0.79$–0.92) between their peak rates. After taking the time shifts between the flash and rainfall rates into consideration, two peaks in the *R* between the mean CG (total) flash and mean rainfall rates in the time windows of 5 (5) and 20 (35) min. An analysis of the two peaks reveals that weak- and moderate-grade SDR events could be correlated with CG flash counts near T_{sus} (i.e., ± 5 min), while SDHR events could be correlated CG flash counts long beyond T_{sus} (i.e., ± 20 min). In particular, higher correlations between total flash rates and rainfall rates could be found in the SDHR events within wider time windows (e.g., up to 35 min). The results indicate that total flashes could be found before rainfall occurrence, thus the total lightning data have the potential of nowcasting SDHR events.

Results also show that the lightning-rainfall correlations vary significantly with different intensity grades. Weak correlations ($R \sim 0.4$) are found in the weak SDR events, and 40–50% of the events are no-flash ones. And moderate correlation ($R \sim 0.6$) are found in the moderate SDR events, and > 10–20% of the events are no-flash ones. In contrast, high correlations ($R \sim 0.7$) are obtained in the SDHR events, and < 10% of the events are no-flash ones. The results indicate that lightning activity is observed more frequently and correlated more robust with the rainfall in the SDHR events. This is understandable because stronger updrafts with large CAPE associated with the SDHR events tend to generate deeper convective clouds with mixed-phase precipitation, providing favorable environments for non-inductive charging process (Matthee et al., 2014), as compared to stratiform clouds with little lightning-precipitation process (Petersen and Rutledge, 1998).

An analysis of the lightning-rainfall correlations in the SDR events with different intensity grades suggest that the rainfall rate thresholds of 2.5 mm $(5\ \text{min})^{-1}$ and 20 mm h^{-1} could be used to discriminate between convective and stratiform rainfall, based on the better correlations that can be achieved. In particular, higher lightning-rainfall correlations could be found when a time shift between the two variables is considered. Specifically, most SDR events could reach their highest correlations if lightning flashes have a time shift within 25 min before and after their durations (T_{sus}). However, lightning-precede-rainfall events account for 50–60% of the total SDR events, whereas lightning-lag-rainfall events account for about 30%. The

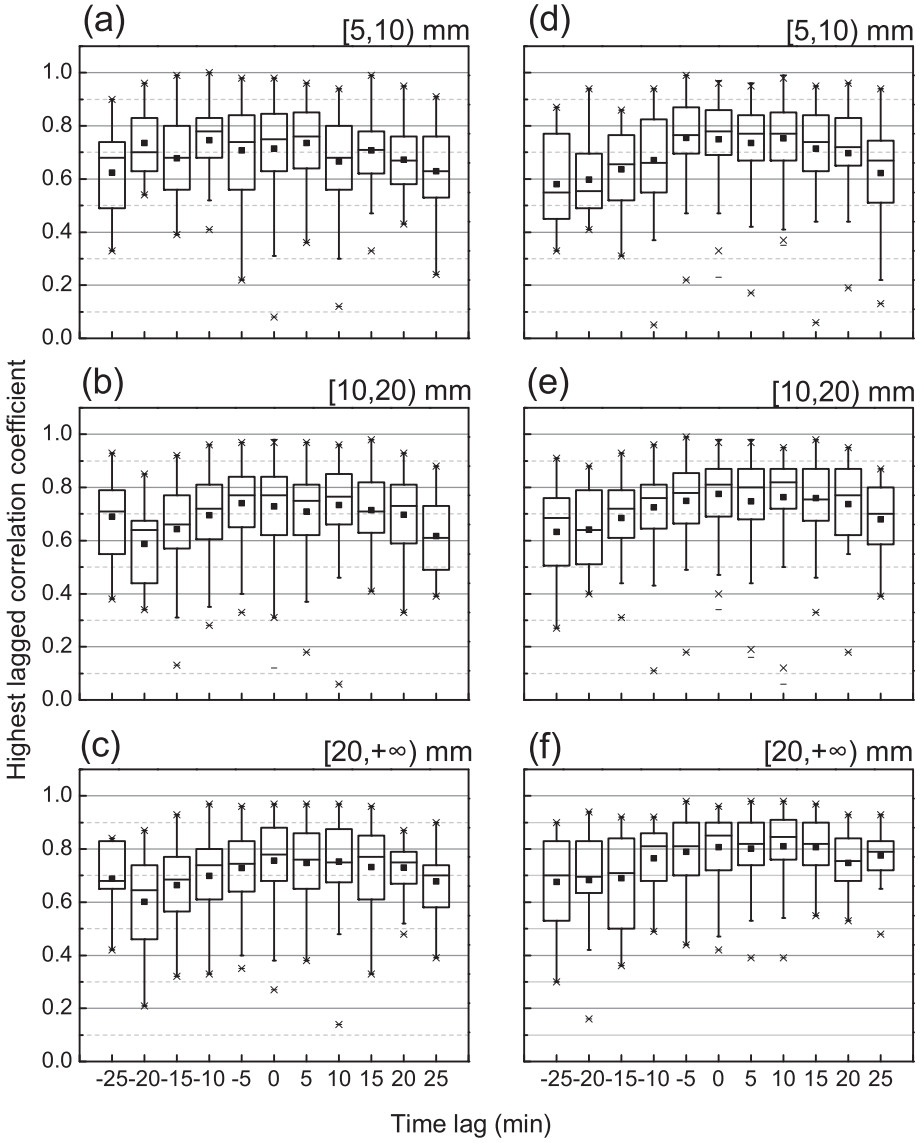

Fig. 12. Box plots of the highest correlation coefficient in the SDR events in the time lags of − 25–25 min. Panels (a)–(c) are for the CG-flash-rainfall correlation associated with the weak SDR, moderate SDR, and SDHR events, respectively; while panels (d)–(f) are the same as panels (a)–(c) but for the total-flash-rainfall correlation.

Table 3
The mean highest correlation coefficient of rainfall and CG flashes [R_{max} (CG)], and the mean highest correlation coefficient of rainfall and total flashes [R_{max} (total)], which are averaged over the SDR events in different intensity grades; the values of test statistic (z); and the percentages of no-flash SDR events observed without any CG [P_0 (CG)] or total [P_0 (total)] lightning flashes.

Intensity	No. of events	R_{max} (CG)	R_{max} (total)	z	P_0 (CG)	P_0 (total)
Weak	1443	0.32	0.40	4.50	52.32	41.51
Moderate	928	0.52	0.62	5.34	23.81	14.12
Intense	554	0.66	0.73	4.43	7.04	4.15

former phenomenon has been understood by the fact that rain reaching to the ground requires several minutes to fall through vertical columns from charged clouds aloft (Piepgrass et al., 1982). However, little has been discussed on the physics behind the time-lagged lightning-rainfall correlation. Thus, more observational studies are much needed to confirm the above findings and explain fully the statistical results obtained herein. The total lightning preceding rainfall phenomenon is especially pronounced for the SDHR events with $R \sim 0.8$. Furthermore, using the total lightning data, the AWSs in the urban areas and northeastern mountainous areas could reach the strong lightning-rainfall correlation of $R = 0.6$–0.8, and even higher at some AWSs in SDHR events. It follows that the total lightning data could be very useful for nowcasting and short-term warning SDHR event. In this regard, previous studies has demonstrated the potential of using lightning data for severe weather warnings, such as tornadoes, hailstorms and wind gusts (Chronis et al., 2015; Schultz et al., 2009, 2011). However, few studies have been conducted to examine the effectiveness of using total lightning data in nowcasting SDHR events. Thus, our results presented herein appear to have important implications for improving the nowcast of SDHR events. Of course, whether or not our results are applicable to all SDHR events occurring in both continental and oceanic regions requires more statistical studies using high-resolution rainfall and lightning observations.

Acknowledgments

This work was supported by the National Basic Research Program of China (973 Program) (Grant No. 2014CB441402). The authors are grateful to Beijing Meteorological Bureau for providing SAFIR-3000 lightning data and AWS rainfall data, and to International Scientific and Technical Data Mirror Site, Computer Network Information Center,

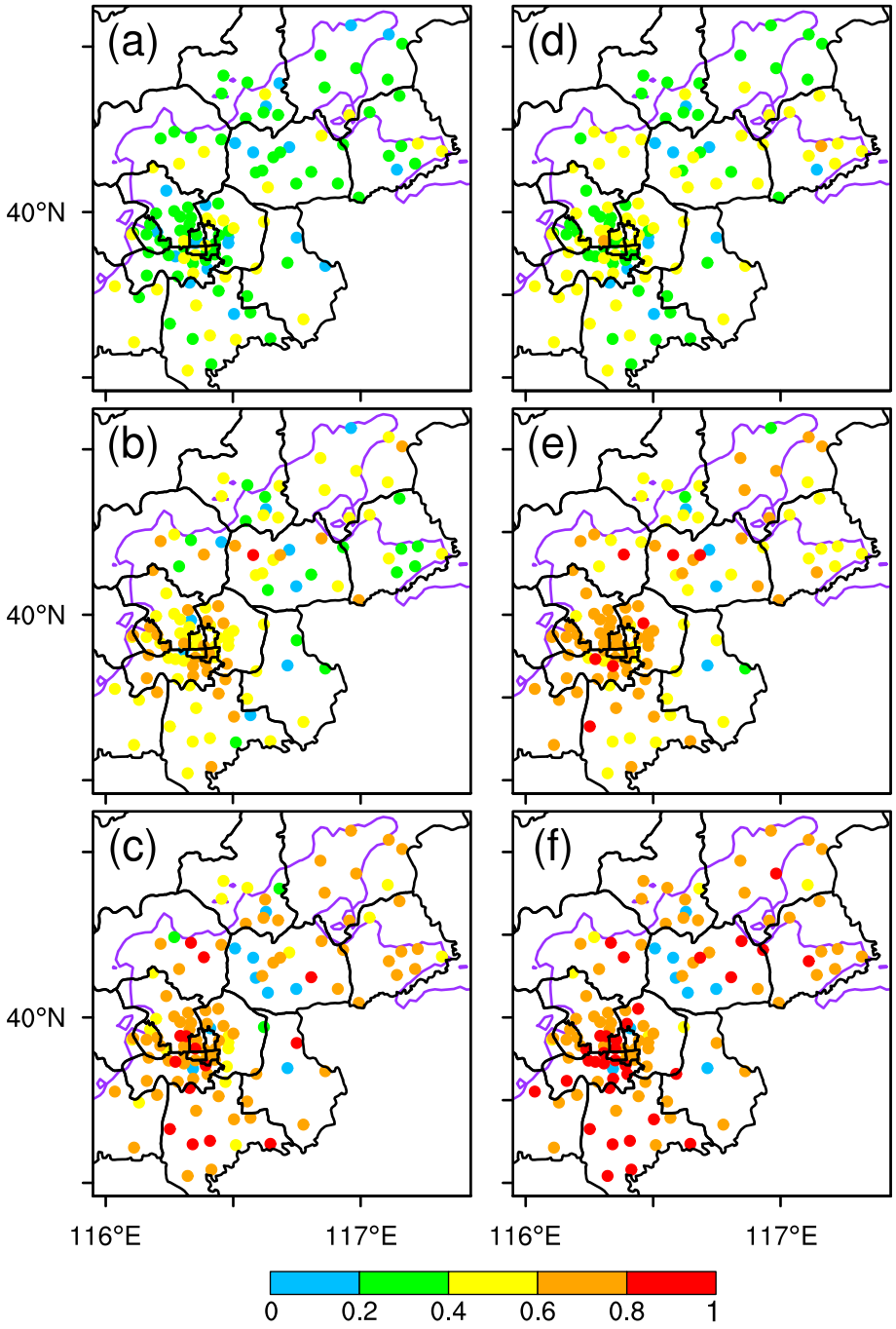

Fig. 13. Spatial distributions of the highest correlation coefficient between rainfall and CG flashes in (a) weak, (b) moderate and (c) heavy SDR events in the time lags of − 60–60 min. Panels (d)–(f) are the same as panels (a)–(c), but for the highest correlation coefficient (*R*) between rainfall and total flashes. Purples lines denote the 200 m terrain elevation.

Chinese Academy of Sciences (http://www.gscloud.cn) for providing the ASTER Global Digital Elevation Model (ASTER GDEM) data.

References

Barnolas, M., Atencia, A., Llasat, M.C., Rigo, T., 2008. Characterization of a Mediterranean flash flood event using rain gauges, radar, GIS and lightning data. Adv. Geosci. 17, 35–41. http://dx.doi.org/10.5194/adgeo-17-35-2008.

Brooks, H.E., Stensrud, D.J., 2000. Climatology of heavy rain events in the United States from hourly precipitation observations. Mon. Weather Rev. 128, 1194–1201. http://dx.doi.org/10.1175/1520-0493(2000)128<1194:COHREI>2.0.CO;2.

Carey, L.D., Rutledge, S.A., 1996. A multiparameter radar case study of the microphysical and kinematic evolution of a lightning producing storm. Meteorog. Atmos. Phys. 59, 33–64. http://dx.doi.org/10.1007/BF01032000.

Carey, L.D., Rutledge, S.A., 2000. The relationship between precipitation and lightning in tropical island convection: a C-band polarimetric radar study. Mon. Weather Rev. 128, 2687–2710. http://dx.doi.org/10.1175/1520-0493(2000)128<2687:TRBPAL>2.0.CO;2.

Chronis, T., Carey, L.D., Schultz, C.J., Schultz, E.V., Calhoun, K.M., Goodman, S.J., 2015. Exploring lightning jump characteristics. Weather Forecast. 30, 23–37. http://dx.doi.org/10.1175/WAF-D-14-00064.1.

Cui, X., Wang, Y., Yu, H., 2015. Microphysical differences with rainfall intensity in severe tropical storm Bilis. Atmos. Sci. Lett. 16, 27–31. http://dx.doi.org/10.1002/asl2.515.

Evans, J.D., 1996. Straightforward Statistics for the Behavioral Sciences. Brooks/Cole Pub Co, Pacific Grove.

Feng, G.L., Qie, X.S., Yuan, T., Niu, S.Z., 2007. Lightning activity and precipitation structure of hailstorms. Sci. China Ser. D Earth Sci. 50, 629–639. http://dx.doi.org/10.1007/s11430-007-2063-8.

Garcia, J.V.C., Stephany, S., d'Oliveira, A.B., 2013. Estimation of convective precipitation mass from lightning data using a temporal sliding-window for a series of thunderstorms in Southeastern Brazil. Atmos. Sci. Lett. 14, 281–286. http://dx.doi.org/10.1002/asl2.453.

Groisman, P.Y., Knight, R.W., Easterling, D.R., Karl, T.R., Hegerl, G.C., Razuvaev, V.N., 2005. Trends in intense precipitation in the climate record. J. Clim. 18, 1326–1350.

http://dx.doi.org/10.1175/JCLI3339.1.
Iordanidou, V., Koutroulis, A.G., Tsanis, I.K., 2016. Investigating the relationship of lightning activity and rainfall: a case study for Crete Island. Atmos. Res. 172–173, 16–27. http://dx.doi.org/10.1016/j.atmosres.2015.12.021.
Jayaratne, E.R., Saunders, C.P.R., Hallett, J., 1983. Laboratory studies of the charging of soft hail during ice crystal interactions. Q. J. R. Meteorol. Soc. 109, 609–630. http://dx.doi.org/10.1002/qj.49710946111.
Katsanos, D., Lagouvardos, K., Kotroni, V., Argiriou, A., 2007. Combined analysis of rainfall and lightning data produced by mesoscale systems in the central and eastern Mediterranean. Atmos. Res. 83, 55–63. http://dx.doi.org/10.1016/j.atmosres.2006.01.012.
Koutroulis, A.G., Grillakis, M.G., Tsanis, I.K., Kotroni, V., Lagouvardos, K., 2012. Lightning activity, rainfall and flash flooding-occasional or interrelated events? A case study in the island of Crete. Nat. Hazards Earth Syst. Sci. 12, 881–891. http://dx.doi.org/10.5194/nhess-12-881-2012.
Piepgrass, M.V., Krider, E.P., Moore, C.B., 1982. Lightning and surface rainfall during Florida thunderstorms. J. Geophys. Res. Ocean. 87, 11193–11201. http://dx.doi.org/10.1029/JC087iC13p11193.
Li, J., Yu, R., Wang, J., 2008. Diurnal variations of summer precipitation in Beijing. Chin. Sci. Bull. 53, 1933–1936. http://dx.doi.org/10.1007/s11434-008-0195-7.
Liu, D., Qie, X., Xiong, Y., Feng, G., 2011. Evolution of the total lightning activity in a leading-line and trailing stratiform mesoscale convective system over Beijing. Adv. Atmos. Sci. 28, 866–878. http://dx.doi.org/10.1007/s00376-010-0001-8.
Liu, D., Qie, X., Pan, L., Peng, L., 2013. Some characteristics of lightning activity and radiation source distribution in a squall line over north China. Atmos. Res. 132–133, 423–433. http://dx.doi.org/10.1016/j.atmosres.2013.06.010.
Matthee, R., Mecikalski, J.R., Carey, L.D., Bitzer, P.M., 2014. Quantitative differences between lightning and nonlightning convective rainfall events as observed with polarimetric radar and MSG satellite data. Mon. Weather Rev. 142, 3651–3665. http://dx.doi.org/10.1175/MWR-D-14-00047.1.
Michaelides, S., Savvidou, K., Nicolaides, K., 2010. Relationships between lightning and rainfall intensities during rainy events in Cyprus. Adv. Geosci. 23, 87–92. http://dx.doi.org/10.5194/adgeo-23-87-2010.
Min, S.-K., Zhang, X., Zwiers, F.W., Hegerl, G.C., 2011. Human contribution to more-intense precipitation extremes. Nature 470, 378–381. http://dx.doi.org/10.1038/nature09763.
Novák, P., Kyznarová, H., 2011. Climatology of lightning in the Czech Republic. Atmos. Res. 100, 318–333. http://dx.doi.org/10.1016/j.atmosres.2010.08.022.
Petersen, W.A., Rutledge, S.A., 1998. On the relationship between cloud-to-ground lightning and convective rainfall. J. Geophys. Res. Atmos. 103, 14025–14040. http://dx.doi.org/10.1029/97JD02064.
Poelman, D.R., 2014. A 10-year study on the characteristics of thunderstorms in Belgium based on cloud-to-ground lightning data. Mon. Weather Rev. 142, 4839–4849. http://dx.doi.org/10.1175/MWR-D-14-00202.1.
Price, C., Federmesser, B., 2006. Lightning-rainfall relationships in Mediterranean winter thunderstorms. Geophys. Res. Lett. 33, 13–16. http://dx.doi.org/10.1029/2005GL024794.
Saunders, C.P.R., Brooks, I.M., 1992. The effects of high liquid water content on thunderstorm charging. J. Geophys. Res. Atmos. 97, 14671. http://dx.doi.org/10.1029/92JD01186.
Saunders, C.P.R., Peck, S.L., 1998. Laboratory studies of the influence of the rime accretion rate on charge transfer during crystal/graupel collisions. J. Geophys. Res. Atmos. 103, 13949–13956. http://dx.doi.org/10.1029/97JD02644.
Schultz, C.J., Petersen, W.A., Carey, L.D., 2009. Preliminary development and evaluation of lightning jump algorithms for the real-time detection of severe weather. J. Appl. Meteorol. Climatol. 48, 2543–2563. http://dx.doi.org/10.1175/2009JAMC2237.1.
Schultz, C.J., Petersen, W.A., Carey, L.D., 2011. Lightning and severe weather: a comparison between total and cloud-to-ground lightning trends. Weather Forecast. 26, 744–755. http://dx.doi.org/10.1175/WAF-D-10-05026.1.
Siegert, S., Bellprat, O., Ménégoz, M., Stephenson, D.B., Doblas-Reyes, F.J., 2017. Detecting improvements in forecast correlation skill: statistical testing and power analysis. Mon. Weather Rev. 145, 437–450. http://dx.doi.org/10.1175/MWR-D-16-0037.1.
Soula, S., Chauzy, S., 2000. Some aspects of the correlation between lightning and rain activities in thunderstorms. Atmos. Res. 56, 355–373. http://dx.doi.org/10.1016/S0169-8095(00)00086-7.
Soula, S., Sauvageot, H., Molinié, G., Mesnard, F., Chauzy, S., 1998. The CG lightning activity of a storm causing a flash-flood. Geophys. Res. Lett. 25, 1181–1184. http://dx.doi.org/10.1029/98GL00517.
Takahashi, T., 1978. Riming electrification as a charge generation mechanism in thunderstorms. J. Atmos. Sci. 35, 1536–1548. http://dx.doi.org/10.1175/1520-0469(1978)035<1536:REAACG>2.0.CO;2.
Tapia, A., Smith, J.A., Dixon, M., 1998. Estimation of convective rainfall from lightning observations. J. Appl. Meteorol. Atmos. 37, 1497–1509. http://dx.doi.org/10.1175/1520-0450(1998)037<1497:EOCRFL>2.0.CO;2.
Taszarek, M., Czernecki, B., Kozioł, A., 2015. A cloud-to-ground lightning climatology for Poland. Mon. Weather Rev. 143, 4285–4304. http://dx.doi.org/10.1175/MWR-D-15-0206.1.
Trenberth, K.E., 2011. Changes in precipitation with climate change. Clim. Res. 47, 123–138. http://dx.doi.org/10.3354/cr00953.
Wang, G., Wang, L., 2013. Temporal and spatial distribution of short-time heavy rain of Beijing in summer (in Chinese). Torrential Rain Disasters 32, 276–279. http://dx.doi.org/10.3969/j.issn.1004-9045.2013.03.012.
Wilks, D.S., 2006. Statistical Methods in the Atmospheric Sciences, second ed. Academic Press, San Diego, California.
Williams, E.R., Weber, M.E., Orville, R.E., 1989. The relationship between lightning type and convective state of thunderclouds. J. Geophys. Res. Atmos. 94, 13213. http://dx.doi.org/10.1029/JD094iD11p13213.
Williams, E.R., Zhang, R., Rydock, J., 1991. Mixed-phase microphysics and cloud electrification. J. Atmos. Sci. 48, 2195–2203. http://dx.doi.org/10.1175/1520-0469(1991)048<2195:MPMACE>2.0.CO;2.
Wu, X., Wang, X., Wang, X., Xu, L., 2000. The effect of urbanization on short duration precipitation in Beijing (in Chinese). J. Nanjing Inst. Meteorol. 23, 68–72. http://dx.doi.org/10.3969/j.issn.1674-7097.2000.01.011.
Wu, F., Cui, X., Zhang, D.-L., Liu, D., Zheng, D., 2016. SAFIR-3000 lightning statistics over the Beijing metropolitan region during 2005–2007. J. Appl. Meteorol. Climatol (JAMC-D-16-0030.1.). http://dx.doi.org/10.1175/JAMC-D-16-0030.1.
Xia, R., Zhang, D.L., Wang, B., 2015. A 6-yr cloud-to-ground lightning climatology and its relationship to rainfall over central and eastern China. J. Appl. Meteorol. Climatol. 54, 2443–2460. http://dx.doi.org/10.1175/JAMC-D-15-0029.1.
Xu, W., Adler, R.F., Wang, N.Y., 2013. Improving geostationary satellite rainfall estimates using lightning observations: underlying lightning-rainfall-cloud relationships. J. Appl. Meteorol. Climatol. 52, 213–229. http://dx.doi.org/10.1175/JAMC-D-12-040.1.
Xu, W., Adler, R.F., Wang, N.Y., 2014. Combining satellite infrared and lightning information to estimate warm-season convective and stratiform rainfall. J. Appl. Meteorol. Climatol. 53, 180–199. http://dx.doi.org/10.1175/JAMC-D-13-069.1.
Yang, P., Ren, G., Hou, W., Liu, W., 2013. Spatial and diurnal characteristics of summer rainfall over Beijing municipality based on a high-density AWS dataset. Int. J. Climatol. 33, 2769–2780. http://dx.doi.org/10.1002/joc.3622.
Yu, R., Xu, Y., Zhou, T., Li, J., 2007. Relation between rainfall duration and diurnal variation in the warm season precipitation over central eastern China. Geophys. Res. Lett. 34, 10–13. http://dx.doi.org/10.1029/2007GL030315.
Yuan, W., Sun, W., Chen, H., Yu, R., 2014. Topographic effects on spatiotemporal variations of short-duration rainfall events in warm season of central North China. J. Geophys. Res. Atmos. 119, 11,223–11,234. http://dx.doi.org/10.1002/2014JD022073.
Zhai, P., Zhang, X., Wan, H., Pan, X., 2005. Trends in total precipitation and frequency of daily precipitation extremes over China. J. Clim. 18, 1096–1108. http://dx.doi.org/10.1175/JCLI-3318.1.
Zhang, D.-L., Lin, Y., Zhao, P., Yu, X., Wang, S., Kang, H., Ding, Y., 2013. The Beijing extreme rainfall of 21 July 2012: right results but for wrong reasons. Geophys. Res. Lett. 40, 1426–1431. http://dx.doi.org/10.1002/grl.50304.
Zhang, L., Wang, M., Li, H., 2015. Discussion of relative accuracy of short-range heavy rain nowcasting (in Chinese). Guangdong Meteorol. 37, 1–6. http://dx.doi.org/10.3969/j.issn.1007-6190.2015.02.001.
Zheng, D., Zhang, Y., Meng, Q., Lü, W., Yi, X., 2009. Total lightning characteristics and electric structure evolution in a hailstorm. ACTA Meteorol. Sin. 233–249. http://dx.doi.org/10.1088/1751-8113/44/8/085201.